JMEPEG (2010) 19:936–941
DOI: 10.1007/s11665-009-9571-y

1059-9495/$19.00

An Analytical Modified Model of Clad Sheet Bonding by Cold Rolling Using Upper Bond Theorem

H. Pishbin, M.H. Parsa, and A. Dastvareh

(Submitted January 17, 2009; in revised form September 6, 2009)

In this paper, clad sheet bonding by cold rolling was investigated using the upper bond theorem. Plastic deformation behavior of the strip at the roll gap was investigated, unlike previous methods; distinctive angular velocities are used for different zones in roll gap in present model and absolute minimum of rolling power function is achieved. Rolling power, rolling force, and thickness ratio of the rolled product affected by various rolling condition such as flow stress of sheets, initial thickness ratio, roller radius, total thickness reduction, coefficient of friction between rollers and metals and between components layer, roll speed, etc., are discussed. It was found that the theoretical prediction of the thickness ratio of the rolled product, rolling force, and rolling power are in good agreement with the experimental measurement.

Keywords clad sheet bonding, cold rolling, cladding, modeling of bimetallic strip, upper bound theorem

1. Introduction

Clad sheets, which consisting of two or more different materials are widely used in various industries due to the induced combined different properties, such as high electrical conductivity, good corrosion resistance, high strength, etc.

The fabrication methods of such composite sheets include diffusion welding, explosion welding, hot pressure welding, hot rolled bonding, and cold-rolled bonding.

Roll bonding is widely used and had been studied by Vaidyanath et al. (Ref 1), Upit and Manik (Ref 2), Wright and Snow (Ref 3), Conrad and Rice (Ref 4), Tylecote et al. (Ref 5), Tylecote and Wynne (Ref 6), Nicholas and Milner (Ref 7), and Bay (Ref 8). Furthermore, Afonja and Sansome (Ref 9), Hyeong and Lee (Ref 10), and Hwang and Tzou (Ref 11) analyzed clad sheet bonding by rolling based on slab analysis method. Hwang and Hsu (Ref 12, 13) and Hwang et al. (Ref 14) based on stream function method, Kiuchi et al. (Ref 15), and Danesh Manesh and Karimi Taheri (Ref 16) based on upper bound theorem, and Lin and Hwang (Ref 17) based on thermal elastic-plastic coupled finite element model had studied clad sheet bonding. They have proposed their own analytical method to examine the plastic deformation behavior in the roll gap.

Current paper is a modified model of Danesh Manesh and Karimi Taheri (Ref 16) model. In the present research, it has been tried to consider all important parameters influencing the cold-rolled cladding process. These parameters are rolling power, rolling force, roll speed, and thickness ratio of the rolled product which is affected by various rolling condition such as flow stress of sheets' material, initial thickness ratio, roller radius, total thickness reduction, coefficient of friction between rollers and strip, and between components layer, etc. Also, unlike Danesh Manesh and Karimi Taheri (Ref 16), in the present model distinctive angular velocities are used for different considered zones in the roll gaps and therefore absolute minimum of rolling power function is achieved.

H. Pishbin, M.H. Parsa, and **A. Dastvareh**, Faculty of Metallurgy and Material Science Engineering, College of Engineering, University of Tehran, P.O. Box 11155/4563, Tehran, Iran. Contact e-mail: Dastvareh@yahoo.com.

Nomenclature	
V_{01}	initial velocity of upper layer
V_{02}	initial velocity of lower layer
V_f	final velocity of bimetal strip
ΔV	amount of velocity discontinuity on each surface of velocity discontinuity
ω_R	rotational velocity of roller
ω	rotational velocity of each rigid zone
U	linear velocity of roll
t_{si}	initial thickness of upper layer
t_{hi}	initial thickness of lower layer
t_{sf}	final thickness of upper layer
t_{hf}	final thickness of lower layer
t_f	final thickness of strip
R_0	roller radius
R	radius of cylindrical surface of velocity discontinuity
r	reduction in area
m_a	coefficient of friction between roller and strip
m_b	coefficient of friction between layers
Γ	surface of velocity discontinuity
S	area of the surface of velocity discontinuity
W	shear power of the surface of velocity discontinuity
σ_s or S_S	flow stress of upper layer
σ_h or S_h	flow stress of lower layer
F	rolling force
L	contact length
J	rolling power
θ	angle between motion direction and X-axis

2. Mathematical Modeling

The proposed model is based on the Danesh Manesh and Karimi Taheri's (Ref 16) model (D-K model) which uses rotating rigid triangle that can be applied to the cold rolling process of bimetal strip. Danesh Manesh and Karimi Taheri (Ref 16) have developed their model using the method presented by Avitzur and Pachala (Ref 18, 19) which has been applied for clad sheet bonding using upper bound theorem. Details of assumed velocity field considered by Avitzur are shown in Appendix A.

Using proposed model and modified upper bound theorem, cold rolling of bimetal strip is analyzed and rolling power, rolling force, and thickness ratio are obtained. The following assumptions are considered in the analysis:

1. The strips behave as rigid plastic material.
2. Deformation in the roll gap is plain strain.
3. Flattening and bending of the rollers are not considered.
4. Bonding of clad sheets is completed after rolling.
5. A constant coefficient of friction is applied between the strips and rollers and components layer.

Figure 1 shows the deformation zones that are divided in six different areas. The magnitude and type of velocities in each zone are different. In zones (I), (II), and (V), the motion are linear and parallel to X-axis ($\theta = 0$). In zones (III), (IV), and (VI), the motion are rotational with two different rotational velocities around roll axis.

In using D-K model for calculating of rotational velocity, it is assumed that rotational velocities in zone (IV) and (VI) are equal. Nevertheless, these neighbor zones have different thicknesses, coefficients of friction, and rotational velocities. In this research, it is assumed that rotational velocity in zone (IV) and (VI) are not equal and according to Avitzur and Pachala (Ref 18) an angular velocity (ω_3) is developed. Angular velocity in zones (III), (IV), and (VI) are shown in Eq 1-3, respectively.

$$V_{01}t_{si} = \int_{R_o}^{r_N} (\omega_1 r)\mathrm{d}r = V_f t_{sf} \tag{Eq 1}$$

$$\frac{V_{02}(t_{hi} - t_{si})}{2} = \int_{r_N}^{r_P} (\omega_2 r)\mathrm{d}r = \frac{V_f(t_{hf} - t_{sf})}{2} \tag{Eq 2}$$

$$\frac{V_{02}(t_{si} + t_{hi})}{2} = \int_{r_P}^{r_N} (\omega_3 r)\mathrm{d}r = \frac{V_f(t_{hf} + t_{sf})}{2} \tag{Eq 3}$$

Required parameters in Eq 1-3 can be calculated using Eq 4-6.

$$r_N = \left\{X_N^2 + (R_0 + t_{sf})^2\right\}^{\frac{1}{2}} \tag{Eq 4}$$

$$r_P = \sqrt{X_P^2 + \left(R_0 + \frac{t_f}{2}\right)^2} \tag{Eq 5}$$

$$r_L = R_o + t_f \tag{Eq 6}$$

Considering Eq 4-6, Eq 1-3 can be converted to:

$$\omega_1 = \frac{2V_{01}t_{si}}{\left(X_N^2 + 2R_0 t_{sf} + t_{sf}^2\right)} = \frac{2V_f t_{sf}}{\left(X_N^2 + 2R_0 t_{sf} + t_{sf}^2\right)} \tag{Eq 7}$$

$$\omega_2 = \frac{V_{02}(t_{hi} + t_{si})}{\left[X_p^2 - X_N^2 + \left(R_0 + \frac{t_f}{2}\right) - (R_0 + t_{sf})^2\right]} = \frac{V_f(t_{hf} - t_{sf})}{\left[X_p^2 - X_N^2 + \left(R_0 + \frac{t_f}{2}\right) - (R_0 + t_{sf})^2\right]} \tag{Eq 8}$$

$$\omega_3 = \frac{V_{02}(t_{si} + t_{hi})}{\left[t_f\left(R_0 + \frac{3}{4}t_f\right) - X_P^2\right]} = \frac{V_f t_f}{\left[t_f\left(R_0 + \frac{3}{4}t_f\right) - X_P^2\right]} \tag{Eq 9}$$

Formulas for calculating radius and surface area of velocity discontinuity are shown in Appendices B and C.

By using Eq 7-9, equations shown in Appendix A, and equations in second column of Appendix B, the velocity ratio $(\varepsilon_i, \lambda_i)$ of the neighboring zones can be determined as presented in Table 1. Velocity discontinuities 1-6 are accordance to D-K model.

Based on the upper bound theorem, total power of plastic deformation in rolling can be expressed as:

$$j = \sum_{i=1}^{g} W_i. \tag{Eq 10}$$

According to the Appendix A, the power losses on the surface of velocity discontinuities such as $\eta_1, \mu_2, \mu_3, \eta_6, \eta_7$, and η_8 can be calculated by using Eq 11.

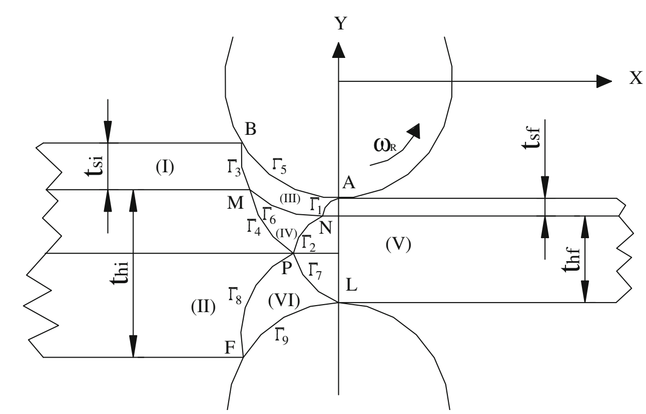

Fig. 1 Velocity discontinuity presented by Danesh Manesh and Karimi Taheri (Ref 16)

Table 1 Velocity ratio in neighbor zones

Number	Velocity ratio
1	$R_1\omega_1$
2	$R_2\omega_2$
3	$R_3\omega_1$
4	$R_4\omega_2$
5	$R_0(\omega_1 - \omega_R)$
6	$R_6(\omega_2 - \omega_1)$
7	$R_7\omega_3$
8	$R_8\omega_3$
9	$R_0(\omega_3 - \omega_R)$

$$W = \left(\frac{\sigma_0}{\sqrt{3}}\right)\Delta V S_s. \quad \text{(Eq 11)}$$

Also power loses in η_5, η_6, and η_9 can be calculated by using of following relation.

$$W = \left(\frac{\sigma_0}{\sqrt{3}}\right)m\Delta V S_s. \quad \text{(Eq 12)}$$

In this model power loses in surfaces Γ_1 to Γ_6 is the same as Danesh Manesh and Karimi Taheri (Ref 16). The upper bound theorem which is presented in Eq 10 is a function of independent parameters such as m_b, m_a, V_f, t_f, t_{hi}, t_{si}, σ_h, σ_s, and V and some dependant parameters such as and X_M, X_P, and X_N are shown in Fig. 1. The five pseudo independent parameters X_M, X_P, X_N, t_{sf}, and V_f are used to minimum the total deformation power. In this point, "for loop method" is used to minimize total deformation power with respect to five pseudo independent parameters X_M, X_P, X_N, t_{sf} and V_f. The "for loop method" is a method for optimizing a loop in a computer program. The loop contains at least a first statement that uses a variable. The method includes inserting a second statement that loads the variable. The second statement is inserted prior to the loop. The method also includes inserting a third statement that (i) checks whether the variable has been written to at any point between the second statement and the third statement and if and only if the variable has been written to, then loading the variable.

The geometric parameters shown in Fig. 1 are restricted to the following range.

$$0.01 < \frac{X_n}{X_b} < 0.1 \quad \text{(Eq 13)}$$

$$0.15 < \frac{X_p}{X_b} < 0.85 \quad \text{(Eq 14)}$$

$$0.9 < \frac{X_m}{X_b} < 0.99 \quad \text{(Eq 15)}$$

and also, range of softer layer thickness is restricted to the following range

$$(1 - r)t_{si}/2 < t_{sf} < t_{si}. \quad \text{(Eq 16)}$$

Lin and Hwang (Ref 17) present the following equation to calculate rolling force and length of contact.

$$F = \frac{JR_0}{LU_0}. \quad \text{(Eq 17)}$$

$$L = \sqrt{Rt_i r}. \quad \text{(Eq 18)}$$

The parameter a in cold roll bonding is assumed to be equal to 0.48 according to Lin and Hwang (Ref 17).

3. Comparison Between Optimum Calculation and Experimental Result of the Rolling Force

Danesh Manesh and Karimi Taheri (Ref 16) have performed some experiments to measure rolling force. Mild steel and Al-tin alloy are used for lower and upper layers and radius and linear velocity of rollers are 75 mm and 362 mm/s, respectively.

Stress-strain relationship for each metal is as follow:

Al-Tin $\bar{\sigma} = 183.1\bar{\varepsilon}^{0.25}$

Mild steel $\bar{\sigma} = 614\,\bar{\varepsilon}^{0.5}$

The coefficient of friction was evaluated indirectly by comparison of the measured rolling power with that calculated ones using present model like Danesh Mansh and Karimi Taheri (Ref 16). In this method, rolling power is computed by using different value of coefficient of friction and reduction in area, and then a coefficient of friction is selected by comparison between calculated rolling power and measured value of rolling power, and these values are presented by Danesh Manesh and Karimi Taheri (Ref 16). Figure 2 shows the effect of area reduction on the required rolling power for the steel/Al-Tin alloy bimetal strip calculated based on two models and measured experimentally. Figure 3 presents the comparison of rolling forces calculated based on the D-K model and the proposed present model with experimental results. This figure illustrates that the rolling force of the bimetal strip is increased with the increase of the total reduction of area.

Furthermore, comparing the experimental results with D-K model's results and also present model's outcomes lead to deduction of frictional coefficient is between strip and rollers. For D-K model and present model, the coefficient of friction were equal to 0.8 and 0.6, respectively.

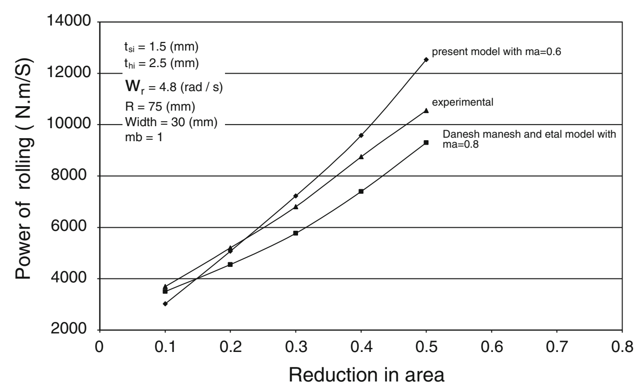

Fig. 2 Effect of reduction in area on rolling power in cold-rolled cladding of bimetallic St-Al/tin strip

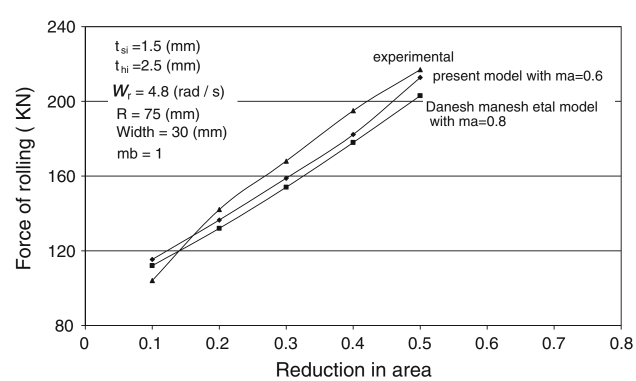

Fig. 3 Effect of reduction in area on rolling force in cold-rolled cladding of bimetallic St-Al/tin strip

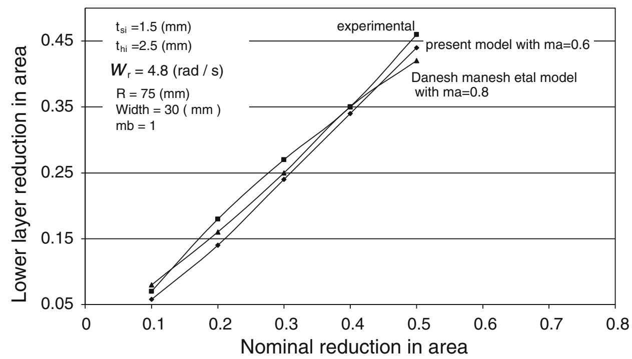

Fig. 4 Effect of reduction in area on the reduction of harder layer in cold-rolled cladding of bimetallic St-Al/tin strip

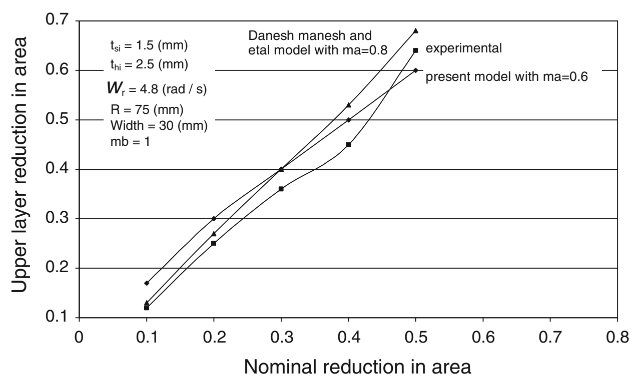

Fig. 5 Effect of reduction in area on the reduction of softer layer in cold-rolled cladding of bimetallic St-Al/tin strip

In the case of D-K model, relative minimum of rolling power was used for calculations while in the present model absolute minimum of rolling power is used.

As mentioned above, the major difference between current research and D-K model is rotational velocity in zone (IV) and (VI). At low reduction of area, the effect of rotation is not so much but by increasing of reduction, the rotation increases and therefore the difference between experiments and calculations increases. According to upper bound theory, analytical value shall be higher than experimental result as shown in Fig. 2 and 3 for current research. In Fig. 4 and 5, the thickness reduction of lower and upper layer after rolling calculated based on D-K model and present model are compared with experimental results. These figures show that the theoretical and experimental results are in good agreement. They also indicate that the reduction of thickness nonuniformly distributed among lower and upper layers at constant thickness reduction of composite strip.

This nonuniform thickness reduction distribution occurred in such way that the reduction of the softer metal is greater than the harder metal. Figures 4 and 5 show the D-K model's results fit to the experimental outcomes by using the frictional coefficient of 0.8. However in the present model, the best fit to the experimental result achieved using the frictional coefficient of 0.6. Note that 0.8 is very high coefficient of friction for cold-rolled metals because it is close to the adhesion friction factor which is equal to 1.

4. Conclusion

In the present model unlike D-K model, distinctive angular velocities are used for different zones in the roll gap. Also in order to optimize the rolling power function, the absolute minimum of rolling power is considered instead of relative minimum was used in D-K model. It is found that the proposed theoretical model can predict rolling power, rolling force, and thickness of each layers of rolled bimetallic strip.

The findings show that there are good agreements between the experimental and the analytical results by assuming the frictional coefficient of 0.6. Rolling power as well as rolling force is increased by increasing the total thickness reduction and increasing of the harder layer thickness. While rolling power and force are decreased by increasing of softer layer thickness. In the case of constant thickness reduction, the thickness reduction of softer layer is greater than harder layer. Figures 2-5 show that in low thickness reductions ranges, D-K model outcomes present better agreement with the experimental results, while in the higher thickness reduction ranges proposed model have better agreement with the experimental results. Also, Fig. 2 and 3 show that angular velocity which presented in D-K model are low and it is better to use lower value of coefficient of friction to analysis bimetallic cold roll cladding. Abovementioned differences between current research and D-K model show that angular velocity in different zone is unequal, so that in order to get a good agreement between analytical models of cold-rolled cladding and experimental results, it had better use different angular velocities in different zones unlike D-K model which different angular velocities are presented above.

Appendix A

A brief of model was presented by Avitzur and Pachala (Ref 18, 19) is shown in Table A1.

Appendix B: Radius of Velocity Discontinuity

Radius of velocity discontinuity for discontinuity 1-6 was presented by Danesh Manesh and Karimi Taheri (Ref 16).

$$R_1 = \left[\frac{X_N^2 + t_{sf}^2}{2t_{sf}}\right]^{0.5}$$

$$R_2 = \left[X_N^2 + \left[R_0 + t_{sf} - \frac{\left[X_P^2 - x_N^2 + \left(R_0 + \frac{t_f}{2}\right)^2 - (R_0 + t_{sf})^2\right]}{(t_f - 2t_{sf})}\right]^2\right]$$

$$R_3 = \left[X_M^2 + \left[\frac{\left(X_N^2 + 2R_0 t_{sf} + t_{sf}^2\right)}{2t_{si}} + R_0 + \frac{t_f - (t_{hi} + t_{si})}{2}\right]^2\right]^{0.5}$$

$$R_4 = \left[X_P^2 + \left[\frac{\left[X_P^2 - X_N^2 + \left(R_0 + \frac{t_f}{2}\right)^2 - (R_0 + t_{sf})^2\right]}{(t_{hi} - t_{si})} + R_0 + \frac{t_f}{2}\right]^2\right]^{0.5}$$

$$R_5 = R_0$$

Table A1 A brief of a model presented by Avitzur and Pachala (Ref 18, 19)

Velocity Field	Axis of surface coordination	Surface radius	Velocity discontinuity	Length of velocity discontinuity	Shear power loses
Both surface have angular motion	$\left(\frac{X_{0I}-\lambda X_{0II}}{1-\lambda}, \frac{Y_{0I}-\lambda Y_{0II}}{1-\lambda}\right)$	$\left[(X_A - X_C)^2 + (Y_A - Y_C)^2\right]^{\frac{1}{2}}$	$R\lvert\omega_1(1-\lambda)\rvert$	$2R\sin^{-1}\frac{\sqrt{(X_A - X_B)^2 + (Y_A - Y_B)^2}}{2R}$ or if $(AB > \pi R)$ $2R\left(\pi - \sin^{-1}\frac{\sqrt{(X_A - X_B)^2 + (Y_A - Y_B)^2}}{2R}\right)$	$\frac{\sigma_0}{3}\Delta VAB$
One surface have linear motion and another have angular motion	$(X_{0I} - \xi\sin\theta_2;$ $Y_{0I} - \xi\cos\theta_2)$		$R\lvert\omega_1\rvert$		

$$R_6 = \left(X_N^2 + R_0^2 + t_{sf}^2 + 2R_0 t_{sf}\right)^{0.5}$$

$$R_7 = \left[R_0 + \frac{\left[t_f\left(R_0 + \frac{3}{4}t_f\right) - X_P^2\right]}{t_f}\right]$$

$$R_8 = \left\{X_P^2 + \left[R_0 + \frac{t_f}{2} + \left[\frac{\left[t_f\left(R_0 + \frac{3}{4}t_f\right) - X_P^2\right]}{(t_{si} + t_{hi})}\right]\right]^2\right\}^{0.5}$$

$$R_9 = R_0$$

Appendix C: Surface Area of Velocity Discontinuity

Surface Area of velocity discontinuity for discontinuity 1-6 was presented by Danesh Manesh and Karimi Taheri (Ref 16).

$$S_1 = 2R_0 a \sin\left[\frac{t_{sf}}{\left(X_N^2 + t_{sf}^2\right)^{0.5}}\right]$$

$$S_2 = 2R_2 a \sin\left[\frac{\left[(X_P - X_N)^2 + \left(\frac{t_f - 2t_{sf}}{2}\right)^2\right]^{0.5}}{2R_2}\right]$$

$$S_3 = 2R_3 a \sin\left\{\frac{\left[\left[\left[R_0^2 - \left[R_0 - \left(\frac{t_{hi} + t_{si} - t_f}{2}\right)\right]^2\right]^{0.5} - X_M\right]^2 + t_{si}^2\right]^{0.5}}{2R_3}\right\}$$

$$S_4 = 2R_4 a \sin\left\{\frac{\left[(X_M - X_P)^2 + \left(\frac{t_{hi} - t_{si}}{2}\right)^2\right]^{0.5}}{2R_4}\right\}$$

$$S_5 = 2R_5 a \sin\left[\left(\frac{t_{si} + t_{hi} - t_f}{4R_5}\right)\right]$$

$$S_6 = 2R_6 a \sin\left\{\frac{\left[(X_N - X_M)^2 + \left[\frac{t_{si} - t_{hi} + (t_f - 2t_{sf})}{2}\right]^2\right]^{0.5}}{2R_6}\right\}$$

$$S_7 = 2R_7 a \sin\left\{\frac{\left[X_P^2 + \left(\frac{t_f}{2}\right)^2\right]^{0.5}}{2R_7}\right\}$$

$$S_8 = 2R_8 a \times \sin\left\{\frac{\left[\left[X_P - \left[R_0^2 - \left[R_0 - \left(\frac{t_{si} + t_{hi} - t_f}{2}\right)\right]^2\right]^{0.5}\right]^2 + \left(\frac{t_{si} + t_{hi}}{2}\right)^2\right]^{0.5}}{2R_8}\right\}$$

$$S_9 = 2R_9 a \sin\left[\left(\frac{t_{si} + t_{hi} - t_f}{4R_9}\right)\right]$$

References

1. L.R. Vaidyanath, M.G. Nicholas, and D.R. Milner, Pressure Welding by Rolling, *Brit. Weld. J.*, 1959, **6**, p 13–28
2. G.U. Upit and J.J. Manik, The Influence of Surface Films on the Pressure Welding of Metals, *Wear*, 1969, **13**, p 77–83
3. P.K. Wright and D.A. Snow, Interfacial Condition and Bond Strength in Cold Pressure Welding by Cold Rolling, *Met. Technol.*, 1978, **20**, p 24–31
4. H. Conrad and L. Rice, The Cohesion of Previously Fractured FCC Metals in Ultrahigh Vacuum, *Metall. Trans.*, 1970, **1**, p 3019–3027
5. R.F. Tylecote, D. Howd, and J.R. Formidge, The Effect of Load on Cohesive Strength of Virgin Surfaces of Plastic Metals, *Weld. J.*, 1958, **5**, p 21–38
6. R.F. Tylecote and E.J. Wynne, Effect of Heat Treatment on Cold Pressure Welds, *Brit. Weld. J.*, 1963, **10**, p 385–391
7. M.J. Nicholas and D.R. Milner, Roll Bonding of Aluminum, *Brit. Weld. J.*, 1962, **11**, p 469–475
8. N. Bay, Cold Welding: Characteristic, Bonding Mechanism and Bond Strength, *Metal Construct.*, 1986, **18**, p 369–372
9. A.A. Afonja and D.H. Sansome, A Theoretical Analysis of the Sandwich Rolling Process, *Int. J. Mech. Sci.*, 1973, **15**, p 1–14
10. S. Hyeong and D.N. Lee, Slab Analysis Method of Roll Bonding of Silver Clad Phosphore Bronze Sheets, *Mater. Sci. Technol.*, 1991, **7**, p 1042–1050
11. Y.M. Hwang and G.Y. Tzou, An Analytical Approach to Asymmetrical Cold and Hot Rolling of Clad Sheet Using the Slab Method, *J. Mater. Process. Technol.*, 1996, **62**, p 249–259
12. Y.M. Hwang and H.H. Hsu, Analysis of Sandwich Sheet Rolling by Stream Function Method, *Int. J. Mech. Sci.*, 1995, **37**, p 297–315
13. Y.M. Hwang and H.H. Hsu, Analysis of Plastic Instability During Sandwich Sheet Rolling, *Int. J. Mach. Tools Manuf.*, 1996, **36**, p 47–62
14. Y.M. Hwang, H.H. Hsu, and Y.L. Hwang, Analytical and Experimental Study on Bonding Behavior at the Roll Gap During Rolling of Sandwich Sheet, *Int. J. Mech. Sci.*, 2000, **42**, p 2417–2434
15. M. Kiuchi, K. Shintani, and Y.M. Hwang, Mathematical Simulation of Cold Sheet Rolling and Sandwich Sheet Rolling, *CIRP*, 1992, **41**, p 289–292
16. H. Danesh Manesh and A. Karimi Taheri, An Investigation of Deformation Behavior and Bonding Strength of Bimetal Strip During Rolling, *Mech. Mater.*, 2005, **37**, p 531–542
17. Z.C. Lin and T.G. Hwang, Different Degree of Reduction and Sliding Phenomenon Study for Three Dimension Hot Rolling with Sandwich Flat Strip, *Int. J. Mech. Sci.*, 2000, **42**, p 1983–2012
18. B. Avitzur and W. Pachala, The Upper Bound Approach to Plane Strain Problem Using Linear and Rotational Velocity Field—Part I: Basic Concept, *J. Eng. Ind.*, 1968, **108**, p 295–306
19. B. Avitzur and W. Pachala, The Upper Bound Approach to Plane Strain Problem Using Linear and Rotational Velocity Field—Part II: Application, *J. Eng. Ind.*, 1968, **108**, p 307–316